Comparison of optomagnetic and AC susceptibility readouts in a magnetic nanoparticle agglutination assay for detection of C-reactive protein

Fock, Jeppe; Parmvi, Mattias; Strömberg, Mattias; Svedlindh, Peter; Donolato, Marco; Hansen, Mikkel Fougt

Published in:
Biosensors and Bioelectronics

Link to article, DOI:
10.1016/j.bios.2016.07.088

Publication date:
2017

Document Version
Peer reviewed version

Comparison of optomagnetic and AC susceptibility readouts in a magnetic nanoparticle agglutination assay for detection of C-reactive protein

Jeppe Fock,[a] Mattias Parmvi,[a,1] Mattias Strömberg,[b] Peter Svedlindh,[b] Marco Donolato, [a,1] and Mikkel Fougt Hansen[a]

[a]*Department of Micro- and Nanotechnology, DTU Nanotech, Technical University of Denmark, Building 345C, DK-2800 Kgs. Lyngby*

[b]*Department of Engineering Sciences, Uppsala University, Box 534, SE-751 21 Uppsala, Sweden*

Corresponding author: Jeppe Fock, +45 45256336

E-mail addresses:

JepF@nanotech.dtu.dk (J. Fock)
Mikkel.Hansen@nanotech.dtu.dk (M.F. Hansen)
Marco@blusense-diagnostics.com (M. Donolato)
Mattias.parmvi@blusense-diagnostics.com (M. Parmvi)
Mattias.Stromberg@angstrom.uu.se (M. Strömberg)
Peter.Svedlindh@angstrom.uu.se (P. Svedlindh)

Abstract

There is an increasing need to develop biosensor methods that are highly sensitive and that can be combined with low-cost consumables. The use of magnetic nanoparticles (MNPs) is attractive because their detection is compatible with low-cost disposables and because application of a magnetic field can be used to accelerate assay kinetics. We present the first study and comparison of the performance of magnetic susceptibility measurements and a newly proposed optomagnetic method. For the comparison we use the C-reactive protein (CRP) induced agglutination of identical samples of 100 nm MNPs conjugated with CRP antibodies. Both methods detect agglutination as a shift to lower frequencies in measurements of the dynamics in response to an applied oscillating magnetic field. The magnetic susceptibility method probes the magnetic response whereas the optomagnetic technique probes the modulation of laser light transmitted through the sample. The two techniques provided highly

[1] Present address: Blusense Diagnostics, Box 68, Fruebjergvej 3,DK-2100 København Ø, Denmark

correlated results upon agglutination when they measure the decrease of the signal from the individual MNPs (turn-off detection strategy), whereas the techniques provided different results, strongly depending on the read-out frequency, when detecting the signal due to MNP agglomerates (turn-on detection strategy). These observations are considered to be caused by differences in the volume-dependence of the magnetic and optical signals from agglomerates. The highest signal from agglomerates was found in the optomagnetic signal at low frequencies.

Keywords
Brownian relaxation, CRP, agglutination assay, magnetic beads, biosensor

1. Introduction

Magnetic nanoparticles (MNPs) provide some unique advantages for use as readout labels in biological assays. For example, MNPs can be forced to move in an applied magnetic field, thereby speeding up reaction kinetics by overcoming limitations imposed by diffusion (Baudry et al., 2006). Further, several sensitive readout principles are available for measurements on MNP suspensions that can be performed without physical or electrical contact to the suspension enabling use of low-cost disposables. Often, the readout is based on a change of the hydrodynamic size of the MNPs in the presence of the target, either due to the target itself binding to the surface of individual MNPs or due to the target-induced clustering of the MNPs. The hydrodynamic size of the MNPs can be obtained in measurements of the Brownian relaxation response of the MNPs, i.e., of the ability of the particles to rotate in response to an oscillating magnetic field (Connolly and St Pierre, 2001).

Initial work utilizing MNPs in a homogeneous assay format focused on the application of a magnetic field to enhance reaction kinetics and measured the change in turbidity at a fixed delay after a magnetic field was applied (Baudry et al., 2006; Moser et al., 2009). In bioassays with a readout based on the Brownian relaxation response of MNPs, the magnetic response from the MNPs was first measured inductively using pickup coils (Astalan et al., 2004; Chung et al., 2004). Later, the magnetic response of suspensions of single domain MNPs was measured optically using the Faraday effect to detect the rotation of polarization of a beam of polarized light (Aurich et al., 2007; Chung et al., 2008; Wilhelm et al., 2002). Subsequent studies found that the optical scattering properties of MNP suspensions in oscillating or rotating magnetic fields resulted in larger signals with reduced requirements for the

magnetic properties of the MNPs as a result (Park et al., 2010; Ranzoni et al., 2011). To distinguish these effects, which have a geometrical origin, from traditional magnetooptical effects, they have been termed "optomagnetic" effects. The optomagnetic effects utilize the linked magnetic and optical anisotropies of the MNPs or clusters of MNPs, i.e., that the scattering and absorption of light by MNPs and clusters of MNPs vary when they rotate in response to an applied oscillating magnetic field. In addition to a larger signal, these approaches greatly simplify the setup and eliminate the need for polarizers.

Although measurements of the magnetic signal have continued to be of interest (Dieckhoff et al., 2014; Engström et al., 2013; Strömberg et al., 2014; Zardán Gómez de la Torre et al., 2011), optomagnetic readout strategies have attracted significant focus (Antunes et al., 2015; Bejhed et al., 2015; Donolato et al., 2015a, 2015b; Mezger et al., 2015; Ranzoni et al., 2012; Tian et al., 2016; Yang et al., 2016). These can be applied on any transparent sample container fitting between the coils providing the magnetic excitation field and therefore they are easily combined with various formats of low-cost disposable sample containers. The assay strategies for the optomagnetic and magnetic readouts are essentially identical, but the two techniques probe very different properties of an MNP suspension and therefore they may respond differently when employed for readout in bioassays. For example, detection of the binding of MNPs to ~1 μm large coils of DNA formed by rolling circle amplification has been performed by both techniques (Donolato et al., 2015a; Strömberg et al., 2014). There, the optomagnetic signal was observed to display a sign change when the circumference of MNP agglomerates approached the wavelength of the laser light and the scattering entered the Mie regime (Bejhed et al., 2015; Donolato et al., 2015a). No sign change was observed for the AC susceptibility data (Strömberg et al., 2014). However, a direct comparison of the two methods has not been presented and it is unclear how agglutination of MNPs affects the signals obtained by the two methods.

Here, we study and compare the two methods when used to read out the response of MNPs with a nominal diameter of 100 nm functionalized with polyclonal CRP antibodies when these are incubated with varying concentrations of CRP in serum. Each CRP molecule has multiple binding sites for the CRP antibodies and can thus result in crosslinking of MNPs as schematically illustrated in Fig. 1. The MNPs have a remnant magnetic moment and rotate in response to an applied magnetic field to

preferentially align the magnetic moment along the applied magnetic field. In an oscillating applied magnetic field, the moments will repeatedly align and randomize during a cycle of the magnetic field. The degree of alignment is determined by the amplitude and frequency of the magnetic field and the Brownian relaxation times of the MNPs. The MNPs used in the present study are irregularly shaped and display linked optical and magnetic anisotropies. Thus, the applied oscillating magnetic field results in a modulation of both the optical scattering properties and the magnetic response of the MNP suspension. The optical response is measured via the modulation of the intensity of light transmitted through the MNP suspension and the magnetic response is measured as the induced voltage in a pick-up coil (Fig. 1). The magnitude and phase of both signals with respect to the magnetic field excitation are measured vs. the frequency, *f*, of the applied magnetic field using lock-in technique. The optomagnetic signal is a geometrical effect and thus depends only on the magnitude of the magnetic field. Therefore, it appears as a signal at 2*f*, i.e., it is detected in the 2nd harmonic signal. The magnetic signal is sensitive to the orientation of the magnetic moment and is detected in the 1st harmonic signal. The frequency response is dominated by Brownian relaxation with a characteristic frequency, f_B, which is inversely proportional to the hydrodynamic volume. Thus, an increase of the hydrodynamic volume of MNPs causes a shift of the response to lower frequencies.

Below, we compare measurements and analysis strategies in a commercially available AC susceptometer and in a setup for optomagnetic measurements using *identical* samples containing various CRP concentrations. This enables a direct comparison of the signals obtained by the two methods. The purpose of the study is to link and compare the two somewhat different but related readout methods to gain insight in the pros and cons of the two methods.

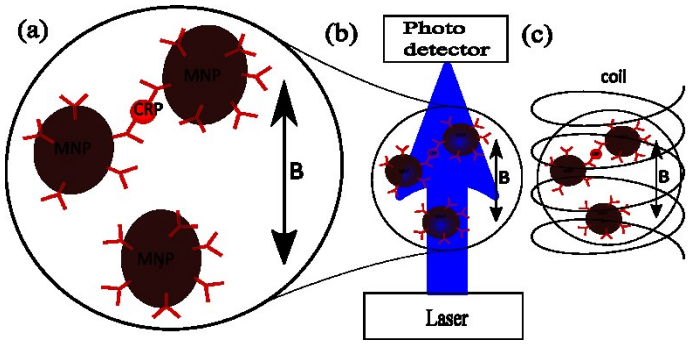

Fig. 1. Schematics of assay and readout principles. (a) The MNPs are functionalized with polyclonal CRP antibodies. CRP molecules can link several MNPs together resulting in formation of clusters (here illustrated for only two MNPs). The orientation of MNPs and of MNP clusters is modulated by application of an oscillating external magnetic field in the vertical direction. (b) The optomagnetic technique measures the modulation of the intensity of the transmitted light using a photodetector. (c) The AC susceptometer measures the voltage in a pick-up coil induced by the time-dependent magnetization variation of the sample.

2. Material and methods

2.1 Functionalization of magnetic nanoparticles

Goat polyclonal CRP antibodies (Abs) (Midland Bioproducts, USA, Product number: 73307) were covalently coupled to 100 nm diameter sized carboxy labeled magnetic nanoparticles (Micromod GmbH, Germany, Prod code: 10-02-102 S04714) using EDC (1-Ethyl-3-(3-dimethylaminopropyl) carbodiimide, Fischer Scientific, Denmark, Product number PI-22980). Unless otherwise stated, all chemicals were purchased from Sigma-Aldrich.

First, stock solutions of MNPs, EDC and Abs were prepared: MNPs were resuspended to 2.5 g/L (2.5 nmol/L) in the conjugation buffer (0.050 mol/L MES, pH 4.8). EDC stock was prepared by dissolving EDC in 0.050 mol/L MES, pH 6.0 to a concentration of 6.4 mmol/L. The Ab stock was concentrated thirty times by spinning the supernatant of the Ab suspension through a centrifugal spin filter with a 30 kDa molecular weight cut off (Amicon Ultra 30MWCO, Merck Millipore, Denmark) to a final concentration of 47.57 g/L (0.3 mmol/L).

Second, the MNPs were functionalized. The Ab stock was spiked to the MNP suspension at a ratio of 12 nm^2 of particle surface per Ab corresponding to 2667 antibodies per MNP (v/v = 2%). Subsequently, the EDC stock was spiked to the suspension at 1000 mol EDC per mol Ab (v/v = 50%). The MNP concentration was adjusted to 0.625 g/L by adding 0.050 mol/L MES, pH 6.0, and the crosslinking reaction proceeded using pulsed vortexing, 1 s on followed by 9 s off, for 30 min at

ambient temperature and was then stopped by adding 25% of the conjugation volume of 0.500 mol/L Tris, 0.500 mol/L Glycine, pH 8.8.

The conjugated MNPs were magnetically separated and washed in wash buffer (0.010 mol/L Tris, 0.05% (v/v) Tween-20, pH 8.9) three times at 1.5 g/L. Finally, the MNPs were blocked using ”The Blocking Solution” (TBS buffer, Candor Bioscience GmbH, Germany, Product number: 110010) for 30 min at ambient temperature at 0.25 g/L (0.25 nmol/L). This suspension formed the stock solution of Ab-functionalized MNPs. The Ab loading was measured to 930 Abs per bead using the absorbance (λ = 280 nm) of the stock solution and of the supernatants from the washing steps.

2.2 Assay

All stock solutions were briefly vortexed before use. 190 µL of the functionalized MNP stock solution was transferred to a cuvette (67.758.001, Sarstedt, Nümbrecht, Germany) and mixed by vortex with 20 µL of CRP-free serum (Hytest Ltd, Finland) spiked with CRP to the indicated concentration, c, of CRP. Note, that c is the CRP concentration in the spiked serum sample and hence that the CRP concentration in the sample after mixing is $0.095c$. The molar mass of CRP is 25106 g/mol. The reaction was allowed to run for 80 min to reach equilibrium. Prior to measurements, the solution was mixed by vortexing.

2.3 Readout

All samples were measured using the optomagnetic setup and subsequently in the commercial AC susceptometer.

2.3.1 Optomagnetic measurements

Optomagnetic measurements were performed on the sample in the cuvette using the system previously described in (Donolato et al., 2015a; Bejhed et al., 2015). In this setup, the magnetic field was applied along the path of the laser light (Sony optical unit, Sony, JP, λ = 405 nm, light beam with a diameter of 2 mm). Two electromagnetic coils (1433428C, Murata Power Solutions Inc., U.S.A.) placed on either side of the cuvette provided a magnetic field excitation with an amplitude of 2.6 mT. The transmission of laser light through the cuvette (2 mm) was measured using a photodiode (PDA36A, Thorlabs Inc., U.S.A.). The magnetic field excitation was controlled and the photodetector signal was recorded via

LabView using a data acquisition card (NI USB-6341, National Instruments, U.S.A.). The 2nd harmonic complex lock-in signal was calculated from the time traces in LabView. The spectra were measured from 1 Hz to 1 kHz in 20 logarithmically equidistant steps. A spectrum was recorded in about 2 min.

2.3.2 Magnetic susceptibility measurements

AC susceptibility measurements were performed using a DynoMag System (Acreo, Swedish ICT, Sweden), which measured the complex magnetic susceptibility in 20 logarithmically equidistant steps from 1 Hz to 100 kHz. The field amplitude was 0.5 mT. The measurements were performed immediately after the optomagnetic measurements where 200 μL of the sample from the cuvette was added to a DynoMag sample container and placed in the instrument. A spectrum was recorded in about 20 min.

3. Results and discussion

Figure 2 shows the results of the optomagnetic and magnetic measurements on 190 μL CRP-Ab functionalized MNPs in buffer and with 20 μL of CRP-free serum spiked with CRP to the indicated concentrations, *c*.

For the optomagnetic (OM) data, the figure shows the in-phase and out-of-phase components, V_2' and V_2'', of the complex 2nd harmonic signal, $V_2 = V_2' + \mathrm{i}V_2'' = |V_2|\left(\cos 2\varphi^{\mathrm{OM}} + \mathrm{i}\sin 2\varphi^{\mathrm{OM}}\right)$, from the photodetector as well as the magnetic phase lag of the signal $\varphi^{\mathrm{OM}} = \mathrm{atan2}\left(-V_2', -V_2''\right)/2$ (Bejhed et al., 2015). The photodetector signals were normalized with respect to the measured average photodetector signal, V_0, to compensate for possible variations in the laser light intensity.

For the AC susceptibility (ACS) data, the figure shows the in-phase and out-of-phase components, χ' and χ'', of the complex magnetic susceptibility signal, $\chi = \chi' - \mathrm{i}\chi'' = |\chi|\left(\cos\varphi^{\mathrm{ACS}} - \mathrm{i}\sin\varphi^{\mathrm{ACS}}\right)$, as well as the magnetic phase lag of the signal, $\varphi^{\mathrm{ACS}} = \mathrm{atan2}\left(\chi'', \chi'\right)$. To account for variation in the MNP concentration from sample to sample, the susceptibility was normalized with respect to the in-phase magnetic susceptibility measured at a high frequency (χ_∞'), which is proportional to the amount of MNPs in the sample (Zardán Gómez de la Torre et al., 2011).

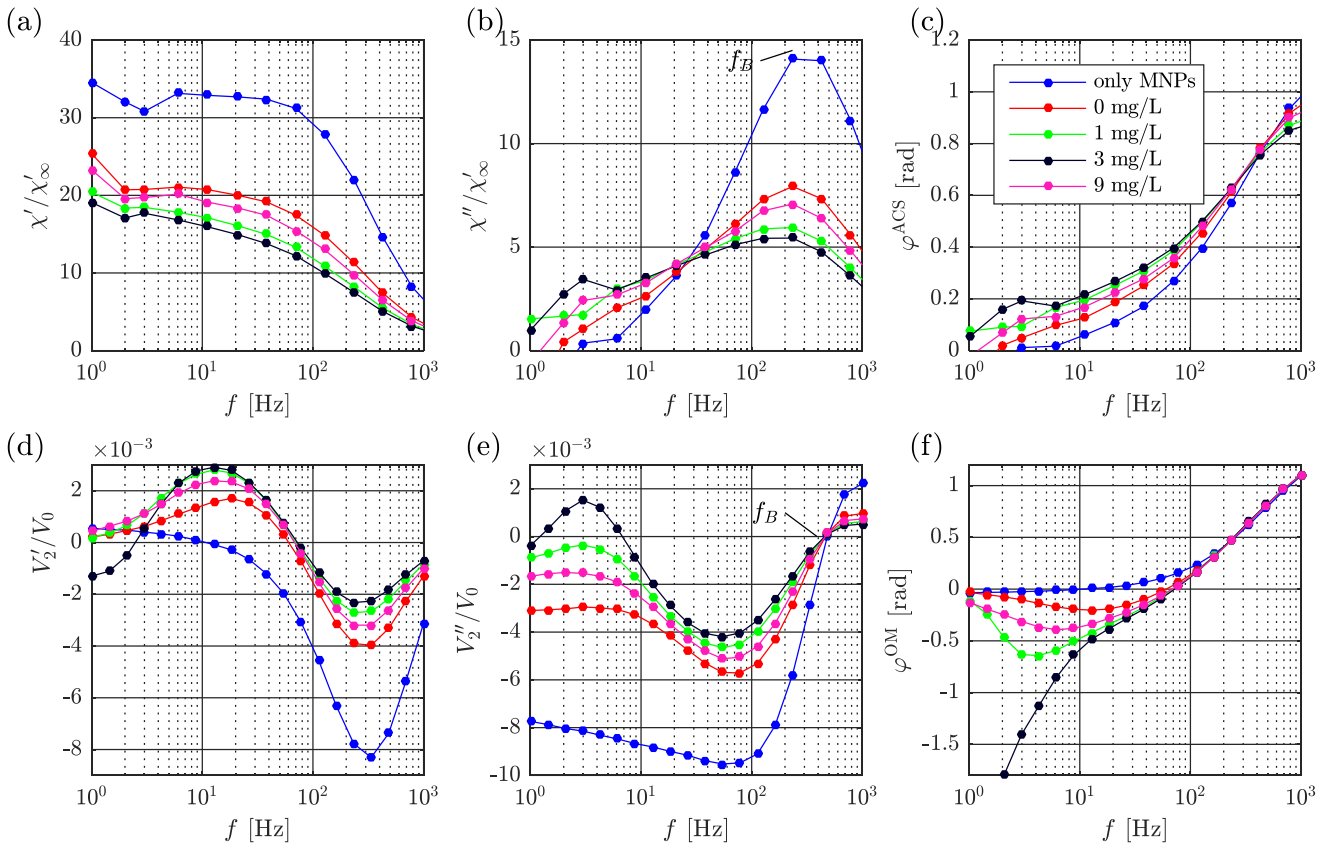

Fig. 2. Results of agglutination assay measurements for anti-CRP functionalized beads in blocking buffer (blue), and in a mixture of 190 µL MNP suspension with 20 µL CRP-free serum with CRP concentrations *c* of <0.02 mg/L (red), 1 mg/L (green), 3 mg/L (black) and 9 mg/L (pink). Panels (a) and (b) show the real and imaginary components χ' and χ'' of the magnetic susceptibility normalized with the high-frequency value of the in-phase susceptibility χ'_∞ and panel (c) shows the corresponding magnetic phase lag $\varphi^{\mathrm{ACS}} = \mathrm{atan2}(\chi'', \chi')$. Panels (d) and (e) show the real and imaginary components V_2' and V_2'' of the optomagnetic signal normalized with the total light intensity V_0 and panel (f) shows the corresponding magnetic phase lag, $\varphi^{\mathrm{OM}} = \mathrm{atan2}(-V_2', -V_2'')/2$. Data in (a)-(c) represent single measurements. Data in (d)-(f) represent three consecutive measurements on the same sample with error bars smaller than the shown data points. The lines are guides to the eye.

3.1 Brownian relaxation of magnetic nanoparticles in buffer

We first compare the observations by the two techniques for the 'only MNPs' sample, where the functionalized MNPs were suspended in blocking buffer with no added serum or CRP. The in-phase magnetic susceptibility, χ' (Fig. 2a), shows a plateau at low frequencies and a decrease towards a small but finite value at high frequencies. The out-of-phase magnetic susceptibility, χ'' (Fig. 2b), shows a peak at a frequency corresponding to the inflection point in the χ' data. This is the typical observation for MNPs exhibiting Brownian relaxation (rotational diffusion).

In the literature it is established that ACS provides the size distribution and that even bi-model distribution can be resolved (Lak et al., 2015). The hydrodynamic size of a monodisperse particle suspension can be found from the χ'' peak position, which corresponds to the Brownian relaxation frequency(Connolly and St Pierre, 2001):

$$f_{\mathrm{B}} = \frac{k_{\mathrm{B}}T}{\pi^2 \eta D_{\mathrm{h}}^3}, \tag{1}$$

where k_{B} is Boltzmann's constant, T is the absolute temperature, η is the dynamic viscosity of the liquid and D_{h} is the hydrodynamic diameter of the MNPs. From analysis of the ACS data in Fig. 2b we obtain $f_{\mathrm{B}}^{\mathrm{ACS}}$= 234 Hz. Using T = 295 K and η = 0.9544 mPa s in Eq. (1), we find $D_{\mathrm{h}}^{\mathrm{ACS}}$= 123 nm.

We have previously argued that for low amplitudes of the magnetic field excitation, the optomagnetic signal can be related to the magnetic susceptibility signal according to

$$V_2' = -\tfrac{1}{\sqrt{2}} V_{\mathrm{ac}} (\tilde{\chi}')(\tilde{\chi}'') \tag{2}$$

$$V_2'' = -\tfrac{1}{2\sqrt{2}} V_{\mathrm{ac}} \left[(\tilde{\chi}')^2 - (\tilde{\chi}'')^2 \right] \tag{3}$$

where $\tilde{\chi} \equiv \chi/\chi_0$ is the susceptibility normalized with respect to the static susceptibility and the amplitude of the time-dependent optomagnetic response V_{ac} is positive when the intensity of transmitted light increases when a magnetic field is applied and negative in the opposite case (Bejhed et al., 2015; Donolato et al., 2015a). Thus, the optomagnetic signal is expected to show a plateau in the V_2'' signal ($\approx -\tfrac{1}{2\sqrt{2}} V_{\mathrm{ac}}$) at low frequencies and a change of sign at $f \approx f_{\mathrm{B}}$, where $\chi' = \chi''$ in a simple Debye model for a single MNP size. Correspondingly, the V_2' signal shows a peak at a frequency related to, but lower than f_{B}. The data in Fig. 2e show that the V_2'' signal shows a plateau-like feature at low frequencies ($f \leq 10^2$ Hz) but also that the signal magnitude continues to decrease when the frequency is lowered. From the optomagnetic data in Fig. 2e, we observe that the V_2'' signal crosses zero at $f_{\mathrm{B}}^{\mathrm{OM}} \approx$ 500 Hz corresponding to $D_{\mathrm{h}}^{\mathrm{OM}} \approx$ 95 nm. However, the magnetic field applied during

these measurements was outside the linear response range for Brownian relaxation and therefore the curves were shifted towards higher frequency (Yoshida and Enpuku, 2009). Therefore, the above value of f_B^{OM} overestimates the true, field-independent, value of f_B^{OM}. Taking this into account, the values of D_h determined by the two methods are consistent with each other and with the manufacturer's specifications. This indicates that both methods can be applied to characterize dispersions of MNPs with a comparatively narrow size distribution.

We attribute the lack of a constant plateau to unspecific agglomeration of MNPs. Due to the larger hydrodynamic size of agglomerates, they contribute to the signal at lower frequencies than the free MNPs. In the magnetic susceptibility measurements, agglomerates are observed as a tail in the signal at low frequencies. In the optomagnetic measurements, agglomerates are also observed at low frequencies, but due to the size-dependence of the optical scattering properties (Donolato et al., 2015a; Yang et al., 2016), these contribute to the signal with a *negative* value of V_{ac} and therefore, according to Eq. (2), a positive signal change is observed at low frequencies (see Figs. 2d and 2e for $f \leq 10^2$ Hz)

3.2 Detection of CRP

Next, we compare the observations by the two techniques for the more complex case where the Ab-functionalized MNPs are mixed with CRP-free serum spiked with CRP at different concentrations. As CRP has multiple binding sites for the polyclonal Abs, each CRP molecule can bind to and link up to two MNPs. In the literature, it has been established that AC susceptibility measurements can be used to estimate the distribution of hydrodynamic size of particles or of clusters of particles via the features in the out-of-phase magnetic susceptibility spectra (Lak et al., 2015). However, it is not a priori clear whether the two very different readout methods provide equivalent information and how the optomagnetic results are influenced by the agglutination of the MNPs. Below, we first describe the general observations by the two methods when adding CRP. Then we analyze the observed changes as function of CRP concentration, and compare results obtained using three different analysis approaches, namely *turn-off detection*, *turn-on detection* and *phase-based detection*.

Figure 2 shows the data measured for CRP-Ab functionalized MNPs mixed with the indicated final concentrations, c, of CRP spiked into CRP-free serum.

We first focus on the magnetic susceptibility data in Figs. 2a-c. In Fig. 2b, it is clearly observed that the peak in the χ'' data at $f = f_B$ for the c = 0 mg/mL sample in serum is reduced in magnitude and broadened towards lower frequencies compared to the 'only MNPs' sample measured in blocking buffer. This difference is attributed to partial agglomeration of the MNPs – either due to unspecific interactions or due to the fact that even CRP-free serum may contain up to 0.02 mg/L CRP. For increasing CRP concentration $c \leq 3$ mg/mL, the peak of the χ'' data in Fig. 2b shows a monotonic decrease in amplitude, a shift towards lower frequencies and a signal appears at frequencies of 10 Hz and below. These changes show a monotonic dependence on c and can unambiguously be attributed to the formation of MNP clusters with increasing hydrodynamic size. For c = 3 mg/L, a clear peak-like feature is observed in the χ'' signal at about 3 Hz corresponding to a hydrodynamic diameter of $D_h^{ACS} \approx$ 500 nm and a hydrodynamic volume, which is about a factor of hundred times larger than that of the individual MNPs. The χ' data in Fig. 2a show a corresponding progression from a nearly flat response at $f < 10^2$ Hz to a reduced signal with a slope of increasing magnitude with increasing c. For c = 9 mg/mL, the magnetic susceptibility data are similar to those obtained for c = 0 mg/mL and c = 1 mg/mL showing that in this case only small MNP clusters have formed. This is attributed to saturation of the individual MNPs with CRP that prevents CRP-mediated linking between MNPs. This well-known 'hook effect' will be discussed in more detail below.

Next, we consider the optomagnetic data in Figs. 2d-f that show a more complex behavior. However, it follows the same systematic dependence on c as the magnetic susceptibility data. We focus at first on the V_2'' data in Fig. 2e. Compared to the 'only MNPs' sample, the c = 0 sample in serum shows a negative signal near $f = 10^2$ Hz, which is reduced in magnitude and superposed with a positive signal at 50 Hz and below. The magnitude of this positive signal increase with c for $c \leq 3$ mg/mL and for c = 3 mg/mL a negative signal change is observed at $f \leq 3$ Hz. The V_2'' spectrum for c = 9 mg/mL lies between those obtained for c = 0 mg/mL and c = 1 mg/mL. Correspondingly, the V_2' data in Fig. 2d show a positive peak that increases in magnitude and shifts from 20 Hz to 15 Hz with increasing c for c

≤ 3 mg/mL and for c = 3 mg/mL, a negative peak in the signal is observed at $f \leq 3$ Hz. The V_2' data for c = 9 mg/mL shows the same behavior as described for the V_2'' data. The above observations can be explained in terms of the dependence of the optical extinction coefficient on the size of agglomerates. The individual MNPs display signal contribution with a positive value of V_{ac}, i.e., more light is transmitted through the MNP suspension when the magnetic field is large. When the MNPs form agglomerates with sizes comparable to the wavelength of the light, the scattering properties change such that less light is transmitted when the magnetic field is large, i.e., V_{ac} becomes negative and the signal changes sign. When very large agglomerates are formed (as observed for c = 3 mg/mL), absorption dominates and the geometrical cross-section of the MNP cluster dominates, which is smaller in an applied magnetic field as the MNP cluster, due to shape anisotropy, will tend to be elongated along the magnetic field and therefore V_{ac} becomes positive again.

The above considerations clearly demonstrate that the two experimental techniques probe different aspects of the properties of the investigated sample and thus it is interesting to compare results obtained using different analysis strategies.

3.3 Dose-response curves and comparison of techniques

Turn-off detection measures the reduction of the signal due to free MNPs when these form agglomerates. This strategy has been employed in several studies that primarily focused on the detection of large amplicons formed by rolling circle amplification of DNA (Donolato et al., 2015a, 2015b; Engström et al., 2013; Strömberg et al., 2014; Zardán Gómez de la Torre et al., 2011). In the present study, we compare the peak value in the out-of-phase magnetic signal, χ''/χ_∞, measured at f = 234 Hz ($\approx f_B$) with the peak value in the optomagnetic signal, V_2'/V_0, measured at f = 334 Hz vs. the CRP concentration, c, in the sample added to the MNP suspension.

Turn-on detection measures the increase of the signal at low frequencies as MNPs form agglomerates. This strategy has been used to a lower extent in previous work (Antunes et al., 2015), as it may be difficult to distinguish the signal from agglomerates from that due to free MNPs. In the present study,

we compare the out-of-phase magnetic signal, χ''/χ_∞, with the optomagnetic signal, V_2'/V_0, measured at $f = 4$ Hz and 12 Hz, respectively.

Phase-based detection measures the changes of the magnetic phase lag for the two signals at one or more frequencies well below f_B, where the phase exhibits a large change upon agglomeration of the MNPs. This approach has the advantage that it is nominally insensitive to small variations in the MNP concentration (Bejhed et al., 2015; Dieckhoff et al., 2014; Mezger et al., 2015). In the present study, we compare the magnetic phase lags, φ^{OM} and φ^{ACS}, determined from the optomagnetic and magnetic susceptibility data measured at $f = 4$ Hz and 12 Hz, respectively.

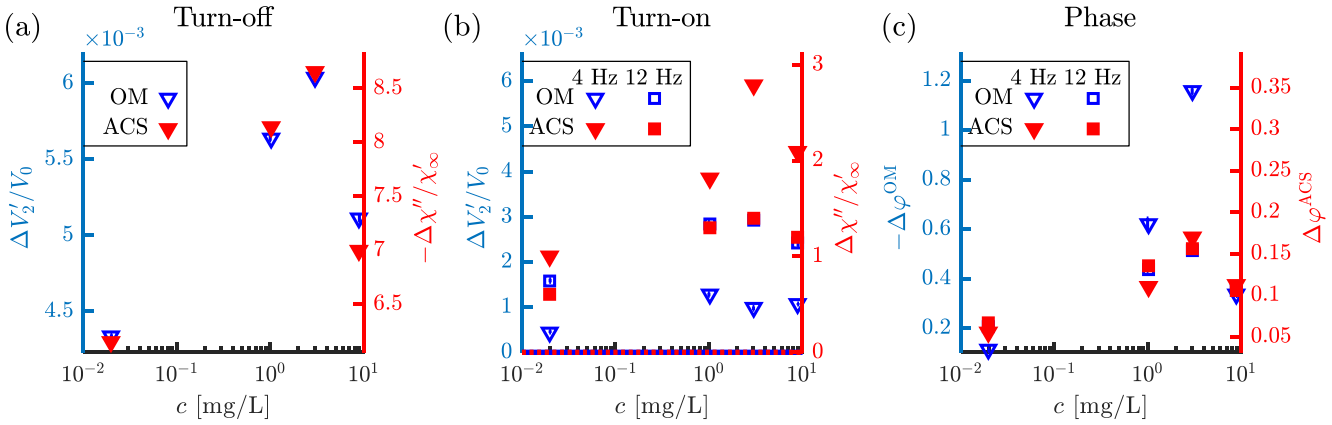

Fig. 3. Dose-response curve for optomagnetic (blue, open symbols) and AC susceptibility measurements (red, filled symbols) obtained using: (a) a *turn-off* scheme measuring the reduction of the single MNP signal at $f = 334$ Hz (OM) and $f = 234$ Hz (ACS); (b) a *turn-on* scheme measuring the signal increase at $f = 4$ Hz (triangles) and 12 Hz (squares); (c) *phase-based* scheme measuring the magnetic phase lag at $f = 4$ Hz (triangles) and 12 Hz (squares). The left and right vertical axes correspond to the OM and ACS data, respectively. All graphs show the signal difference compared to the MNP sample in blocking buffer. The points at 0.02 mg/L correspond to CRP-free serum ($c < 0.02$ mg/L). AC susceptibility measurements were performed in singlet. Error bars for the OM data were obtained from three consecutive measurements on the same sample.

Figures 3a-c show the signals vs. c for the three above analysis strategies. All values are shown relative to the signal from the MNPs in buffer (the 'only beads' sample), and the upper values of the scales have been chosen to obtain the best overlap of data.

For the *turn-off* dose-response curve (Fig. 3a) there is a good general agreement between the optomagnetic and magnetic susceptibility values, which is reflected in a Pearson correlation coefficient,

r, of 0.9991. For the *turn-on* detection, on the other hand, the selection of probe frequency has a large impact on the results. We attribute this to the change of the size distribution for the different CRP concentrations and that the agglomerate sizes are weighted differently in the two methods. The AC susceptibility signal is weighted by the square of the magnetic moment of the agglomerates, which may show a non-trivial dependence on the agglomerate size. The optomagnetic signal is also weighted by the square of the magnetic moment, but furthermore by the extinction properties of the agglomerates, which are known to depend strongly on the size. The aspect ratio of agglomerates and the distribution of MNP orientations within an agglomerate are not known and may potentially depend on the size of the agglomerate. In addition, the sign of the optomagnetic signal changes twice with increasing size of the agglomerates. For the 12 Hz *turn-on* detection (Fig. 3b), we obtain a larger correlation between the two methods (r = 0.99) compared to the 4 Hz *turn-on* detection (r = 0.86). We hypothesize the reason for this to be that agglomerates with similar scattering properties (positive V_2'/V_0 signal) contribute mostly to the optomagnetic signal near f = 12 Hz, whereas for f > 12 Hz also the free MNPs contribute with a negative signal such that the resulting signal is due to a size distribution with mixed positive and negative signals. Correspondingly, for f < 12 Hz a negative signal from the very large agglomerates contributes and the signal again is due to a mixture of positive and negative signals.

The change in the magnetic phase lag obtained from the magnetic susceptibility data is almost independent on f for f < 100 Hz when the MNPs agglomerate (Fig. 2c). This is reflected in the *phase-based* detection data (Fig. 3b) that overlap for 4 Hz and 12 Hz. In contrast, the magnetic phase lag determined from the optomagnetic data is strongly sensitive to both the frequency and the agglomeration state. At f = 12 Hz, φ^{OM} resembles φ^{ACS}, but φ^{OM} differs significantly from φ^{ACS} at lower frequencies (Fig. 2f). As discussed above, these differences are attributed to different weighting of the size distributions in the two methods. The sign changes in the optomagnetic signal make the magnetic phase difficult to interpret physically because the signal is a superposition of contributions with different signs and the calculation of the phase is non-linearly related to these contributions. However, as observed in Fig. 3c, a large change in the phase is observed at low frequencies (4 Hz). This indicates that the phase of the optomagnetic signal is highly sensitive to formation of agglomerates.

We next consider the 'hook effect' that occurs when MNPs approach saturation with CRP such that CRP-mediated MNP agglomeration is reduced. The highest response observed at c = 3 mg/L CRP corresponding to 50 CRP molecules per MNP. For c = 9 mg/L (150 CRP molecules per MNP), the response is reduced indicating that the MNPs become partially blocked by CRP molecules and hence are less able to agglomerate. The CRP concentration above which the hook effect appears can be modified by changing the MNP concentration, the number of active Abs per MNP or by diluting the sample. Such changes can also be used to tune the lower range of concentrations that can be resolved.

To further support the validity of the above comparison and conclusions concerning the different readout strategies, we carried out the same analysis and comparison for the CRP assay in Tris buffer at pH 9 (SI, Section S1). The higher pH decreased the affinity of anti-CRP towards CRP. Therefore, the hook effect was shifted to a higher CRP concentration. Despite these differences, we observed the same relations between the magnetic and optomagnetic measurements as described above.

The present study focused on the comparison of the optomagnetic and magnetic susceptibility readouts on identical samples with different degrees of MNP clustering, where CRP was used as a test case. The results suffered from partial MNP agglomeration due to unspecific interactions and/or a small amount of CRP in the nominally CRP free serum sample, which would have to be resolved to assess the limit of detection of the techniques on clinical samples. The reduction of this agglomeration is topic of our further work.

5. Conclusion

We have compared an optomagnetic readout to a more established magnetic readout of the distribution of hydrodynamic sizes of magnetic nanoparticles using a CRP agglutination assay as a test case. The measurements, which were performed sequentially on the *same* samples, showed excellent correlation when used in a turn-off detection scheme based on monitoring the depletion of free MNPs. The high correlation between the methods shows that the two methods in that case probe the same Brownian relaxation dynamics. However, using turn-on and phase-based detection schemes, the correlation between the two techniques is less clear because the two methods have different sensitivities to the size of agglomerates. In the magnetic susceptibility measurements, agglomerates were observed as a shoulder on the free MNP signal, whereas in the optomagnetic measurements, agglomerates were

observed as signals with opposite sign of that due to free MNPs. Further, the optomagnetic technique was more sensitive to large agglomerates. The optomagnetic technique had the advantage that measurements were completed in a matter of minutes compared to tens of minutes for the commercial AC susceptometer. The main reason for this is that the magnetic signal in the susceptometer is proportional to the frequency and hence is weak at low frequencies, where a longer measurement time is needed to obtain sufficient data quality. Further, the inherent higher sensitivity of the optical signal enables measurements at lower MNP concentrations where a higher sensitivity may be achieved. Finally, the optomagnetic setup is simple, compatible with plastic disposable sample containers and it can be constructed using low-cost hardware components.

Acknowledgements

This work is financially supported by EU FP7 grant No. 604448-NanoMag and the Swedish Research Council Formas Project No. 221-2012-444.

References

Antunes, P., Watterson, D., Parmvi, M., Burger, R., Boisen, A., Young, P., Cooper, M.A., Hansen, M.F., Ranzoni, A., Donolato, M., 2015. Quantification of NS1 dengue biomarker in serum via optomagnetic nanocluster detection. Sci. Rep. 5, 16145. doi:10.1038/srep16145

Astalan, A.P., Ahrentorp, F., Johansson, C., Larsson, K., Krozer, A., 2004. Biomolecular reactions studied using changes in Brownian rotation dynamics of magnetic particles. Biosens. Bioelectron. 19, 945–951. doi:10.1016/j.bios.2003.09.005

Aurich, K., Nagel, S., Glöckl, G., Weitschies, W., 2007. Determination of the magneto-optical relaxation of magnetic nanoparticles as a homogeneous immunoassay. Anal. Chem. 79, 580–586. doi:10.1021/ac060491r

Baudry, J., Rouzeau, C., Goubault, C., Robic, C., Cohen-Tannoudji, L., Koenig, a, Bertrand, E., Bibette, J., 2006. Acceleration of the recognition rate between grafted ligands and receptors with magnetic forces. Proc. Natl. Acad. Sci. U. S. A. 103, 16076–16078. doi:10.1073/pnas.0607991103

Bejhed, R.S., Zardán Gómez de la Torre, T., Donolato, M., Hansen, M.F., Svedlindh, P., Strömberg, M., 2015. Turn-on optomagnetic bacterial DNA sequence detection using volume-amplified magnetic nanobeads. Biosens. Bioelectron. 66, 405–411. doi:10.1016/j.bios.2014.11.048

Chung, S.-H., Grimsditch, M., Hoffmann, A., Bader, S.D., Xie, J., Peng, S., Sun, S., 2008. Magneto-optic measurement of Brownian relaxation of magnetic nanoparticles. J. Magn. Magn. Mater. 320, 91–95. doi:10.1016/j.jmmm.2007.05.016

Chung, S.H., Hoffmann, A., Bader, S.D., Liu, C., Kay, B., Makowski, L., Chen, L., 2004. Biological sensors based on Brownian relaxation of magnetic nanoparticles. Appl. Phys. Lett. 85, 2971–2973.

doi:10.1063/1.1801687

Connolly, J., St Pierre, T.G., 2001. Proposed biosensors based on time-dependent properties of magnetic fluids. J. Magn. Magn. Mater. 225, 156–160. doi:10.1016/S0304-8853(00)01245-2

Dieckhoff, J., Lak, A., Schilling, M., Ludwig, F., 2014. Protein detection with magnetic nanoparticles in a rotating magnetic field. J. Appl. Phys. 115, 024701. doi:10.1063/1.4861032

Donolato, M., Antunes, P., Bejhed, R.S., Zardán Gómez de la Torre, T., Østerberg, F.W., Strömberg, M., Nilsson, M., Strømme, M., Svedlindh, P., Hansen, M.F., Vavassori, P., 2015a. Novel Readout Method for Molecular Diagnostic Assays Based on Optical Measurements of Magnetic Nanobead Dynamics. Anal. Chem. 87, 1622–1629. doi:10.1021/ac503191v

Donolato, M., Antunes, P., Zardán Gómez de la Torre, T., Hwu, E.-T., Chen, C.-H., Burger, R., Rizzi, G., Bosco, F.G., Strømme, M., Boisen, A., Hansen, M.F., 2015b. Quantification of rolling circle amplified DNA using magnetic nanobeads and a Blu-ray optical pick-up unit. Biosens. Bioelectron. 67, 649–655. doi:10.1016/j.bios.2014.09.097

Engström, A., Zardán Gómez de la Torre, T., Strømme, M., Nilsson, M., Herthnek, D., 2013. Detection of Rifampicin Resistance in Mycobacterium tuberculosis by Padlock Probes and Magnetic Nanobead-Based Readout. PLoS One 8, e62015. doi:10.1371/journal.pone.0062015

Lak, A., Thünemann, A.F., Schilling, M., Ludwig, F., 2015. Resolving particle size modality in bi-modal iron oxide nanoparticle suspensions. J. Magn. Magn. Mater. 380, 140–143. doi:10.1016/j.jmmm.2014.08.050

Mezger, A., Fock, J., Antunes, P., Østerberg, F.W., Boisen, A., Nilsson, M., Hansen, M.F., Ahlford, A., Donolato, M., 2015. Scalable DNA-Based Magnetic Nanoparticle Agglutination Assay for Bacterial Detection in Patient Samples. ACS Nano 9, 7374–7382. doi:10.1021/acsnano.5b02379

Moser, Y., Lehnert, T., Gijs, M.A.M., 2009. On-chip immuno-agglutination assay with analyte capture by dynamic manipulation of superparamagnetic beads. Lab Chip 9, 3261. doi:10.1039/b907724c

Park, S.Y., Handa, H., Sandhu, A., 2010. Magneto-optical biosensing platform based on light scattering from self-assembled chains of functionalized rotating magnetic beads. Nano Lett. 10, 446–451. doi:10.1021/nl9030488

Ranzoni, A., Sabatte, G., van IJzendoorn, L.J., Prins, M.W.J., 2012. One-Step Homogeneous Magnetic Nanoparticle Immunoassay for Biomarker Detection Directly in Blood Plasma. ACS Nano 6, 3134–3141. doi:10.1021/nn204913f

Ranzoni, A., Schleipen, J.J.H.B., van IJzendoorn, L.J., Prins, M.W.J., 2011. Frequency-Selective Rotation of Two-Particle Nanoactuators for Rapid and Sensitive Detection of Biomolecules. Nano Lett. 11, 2017–2022. doi:10.1021/nl200384p

Strömberg, M., Zardán Gómez de la Torre, T., Nilsson, M., Svedlindh, P., Strømme, M., 2014. A magnetic nanobead-based bioassay provides sensitive detection of single- and biplex bacterial DNA using a portable AC susceptometer. Biotechnol. J. 9, 137–145. doi:10.1002/biot.201300348

Tian, B., Bejhed, R.S., Svedlindh, P., Strömberg, M., 2016. Blu-ray optomagnetic measurement based competitive immunoassay for Salmonella detection. Biosens. Bioelectron. 77, 32–39. doi:10.1016/j.bios.2015.08.070

Wilhelm, C., Gazeau, F., Roger, J., Pons, J.N., Salis, M.F., Perzynski, R., Bacri, J.C., 2002. Binding of biological effectors on magnetic nanoparticles measured by a magnetically induced transient birefringence experiment. Phys. Rev. E 65, 031404. doi:10.1103/PhysRevE.65.031404

Yang, J., Donolato, M., Pinto, A., Bosco, F.G., Hwu, E.-T., Chen, C.-H., Alstrøm, T.S., Lee, G.-H., Schäfer, T., Vavassori, P., Boisen, A., Lin, Q., Hansen, M.F., 2016. Blu-ray based optomagnetic aptasensor for detection of small molecules. Biosens. Bioelectron. 75, 396–403. doi:10.1016/j.bios.2015.08.062

Yoshida, T., Enpuku, K., 2009. Simulation and quantitative clarification of AC susceptibility of magnetic fluid in nonlinear Brownian relaxation region. Jpn. J. Appl. Phys. 48. doi:10.1143/JJAP.48.127002

Zardán Gómez de la Torre, T., Mezger, A., Herthnek, D., Johansson, C., Svedlindh, P., Nilsson, M., Strømme, M., 2011. Detection of rolling circle amplified DNA molecules using probe-tagged magnetic nanobeads in a portable AC susceptometer. Biosens. Bioelectron. 29, 195–199. doi:10.1016/j.bios.2011.08.019